

Model-based fault detection of blade pitch system in floating wind turbines

S Cho^{1,2}, Z Gao^{1,2} and T Moan^{1,2}

¹ Department of Marine Technology, Norwegian University of Science and Technology (NTNU), Trondheim, Norway.

² Centre for Autonomous Marine Operations and Systems (AMOS), Norwegian University of Science and Technology (NTNU), Trondheim, Norway.

Corresponding author's e-mail address: seongpil.cho@ntnu.no

Abstract. This paper presents a model-based scheme for fault detection of a blade pitch system in floating wind turbines. A blade pitch system is one of the most critical components due to its effect on the operational safety and the dynamics of wind turbines. Faults in this system should be detected at the early stage to prevent failures. To detect faults of blade pitch actuators and sensors, an appropriate observer should be designed to estimate the states of the system. Residuals are generated by a Kalman filter and a threshold based on H_∞ optimization, and linear matrix inequality (LMI) is used for residual evaluation. The proposed method is demonstrated in a case study that bias and fixed output in pitch sensors and stuck in pitch actuators. The simulation results show that the proposed method detects different realistic fault scenarios of wind turbines under the stochastic external winds.

1. Introduction

Maintenance and repair of offshore wind turbines are challenging because of the difficult access. Especially, faults occur unexpectedly in components of wind turbines such as blades, drivetrain or generator. Faults in wind turbines can directly influence the operational safety, dynamics and power production efficiency of wind turbines. An early-stage fault diagnosis technique should be conducted regarding maintenance and repair to prevent loss of energy production and economic values of wind turbines with active fault accommodation. Therefore, there is a growing demand for fault-tolerant control which can be achieved an efficient fault diagnosis and accommodation.

The blade pitch system is crucial to adjust the blade pitch angle for controlling rotor speed, aerodynamic force, torque, and power. The main faults of the blade pitch system occur in its blade pitch sensor and actuator. These faults influence control feedback and result in imbalance loads on the rotor, shaft, and the main bearings. The detection of faults allows for fast accommodation to avoid catastrophic long term damages in the wind turbines.

A model-based fault detection method comprises residual generation and evaluation based on a threshold method [1][2]. The residual signal must be close to zero in a normal condition. In a model-based approach, the faults are detected typically by a residual signal, the value of which must be greater than zero in a fault condition. The threshold based on the H_∞ norm that represents a maximum effect of the disturbance was employed by Zhang et al. [2]. Also, linear matrix inequality (LMI) was used to determine the optimal H_∞ norm and to design a robust fault detection observer [2].



Sensor fault detection and isolation in the blade pitch system, generator shaft and converter were simulated by Odgaard et al. [3]. Chen et al. [4] applied observer-based FDI schemes to the model presented by [3]. The simulations in those studies were performed in frequency domain analyses that have limitations on fast detection of the pitch sensor and actuator faults. Wang et al. [5] used a time-domain approach that ensured fast fault detection for floating wind turbines.

This paper deals with a fault detection method in blade pitch sensors and actuators of a wind turbine model by using Kalman filter. The case study is based on the NREL 5MW wind turbine model [6] supported by the spar buoy floater (OC3 Hywind) [7]. The dynamic behavior of the wind turbine model is simulated by using Simo-Riflex-Aerodyn (SRA) [8] and external control code for a PI pitch and torque controller. A subroutine is added to SRA to account for pitch actuator and sensor. The observer based on Kalman filter estimates the states of the system based on a mathematical model, sensor measurements, and input commands. Faults generated in blade pitch sensors and actuators can be detected by this observer based on residual generation and evaluation method by using a threshold. Faults in the blade pitch system are given in the input file of SRA to test the feasibility of the fault detection. Fault magnitude, type and occurrence time are decided in advance. The optimal threshold is computed by H_∞ norm and the LMI approach.

This paper is organized as follows: Section 2 describes the blade pitch system consisted of the baseline controller, pitch actuator, and pitch sensor. In Section 3 fault detection schemes of the blade pitch system are introduced with Kalman filter, H_∞ norm and the LMI approach for threshold design. In Section 4, simulation results for the fault detection technique are presented by a residual method and fault decision by a fault detection criterion. The conclusions are presented in Section 5.

2. Blade pitch system

Wind turbines should be designed to maximize generated power and ensure continued reliability during operation. The operational region from the cut-in wind speed to the cut-out wind speed is divided into below-rated (Region II) and above-rated regions (Region III) of wind speed as illustrated in Figure 1. In order to optimize the productivity of a wind turbine in Region II and III, its power output must be maximized from the cut-in wind speed (V_{cut-in} , 3m/s) to the rated wind (V_{rated} , 11.4m/s) in Region II and constant until the cut-out wind speed ($V_{cut-out}$, 25m/s) in Region III achieved by adjusting the blade pitch angle and controlling generator torque with blade pitch and torque controller. A blade pitch system mainly comprises a PI controller, pitch actuator and pitch sensor.

2.1. Baseline Control system

The baseline control system includes two separate controllers for regulating blade pitch angles and generator torque, respectively. In Region II, the control strategy is to capture the maximum power by maintaining optimal tip speed ratio [6]. The generator torque is inversely proportional to the filtered generator speed. Within this region, the blade pitch controller is not active and maximum power is achieved by adjusting the generator torque.

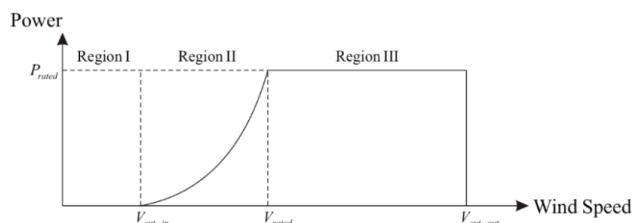


Figure 1. Ideal power curve as a function of the wind speed

In Region III, a constant torque variable pitch controller is used for floating wind turbines regarding stability issue [9] by modified gains of the controller. A blade pitch reference $\beta_{ref}(t)$ is computed based on gain-scheduled proportional-integral (PI) controller as the function of the generator torque error $e(t)$ based on a constant-torque strategy [10] in floating wind turbines.

$$\beta_{ref}(t) = K_P(\beta)e(t) + K_I(\beta)\int_0^t e(t)dt, \quad e(t) = f(\tau_{g,ref} - \tau(t)) \quad (1)$$

The blade pitch control system of the wind turbine regulates the blade pitch angle and the generator speed. The values of control gains are described as follows

$$K_P(\beta) = GK(\beta)K_{P,0}, \quad K_I(\beta) = GK(\beta)K_{I,0}, \quad GK(\beta) = 1/(1 + \beta/K_K) \quad (2)$$

where $K_P(\beta)$ is the proportional gain, $K_I(\beta)$ is the integration gain, $GK(\beta)$ is the gain correction factor, K_K is the pitch angle where the gain function is equal to 0.5 for the NREL 5MW wind turbine [6].

Using the properties for the recommended response characteristics, the resulting gains are $K_{P,0} = 0.0188268s$, $K_{I,0} = 0.00806863$, and $K_K = 0.11$ [6]. The pitch rate limit is set from -8 to $8^\circ/s$ based on General Electric (GE)'s long-blade test program. Also, the pitch range is also set from 0° to 90° . Figure 2 shows a block diagram of the baseline control system that can represent how the system interacts the blade pitch system with other systems by measuring the generator speed and pitch angle. The parameters can be described in Figure 2 that Ω_r is the rotor speed, Ω_g is the generator speed, $\Omega_{g,m}$ is the measured generator speed, $\Omega_{g,rated}$ is the rated generator speed, τ_g is the generator torque, τ_a is the aerodynamic torque, and β_m is the measured blade pitch angle, and V_w is the wind speed.

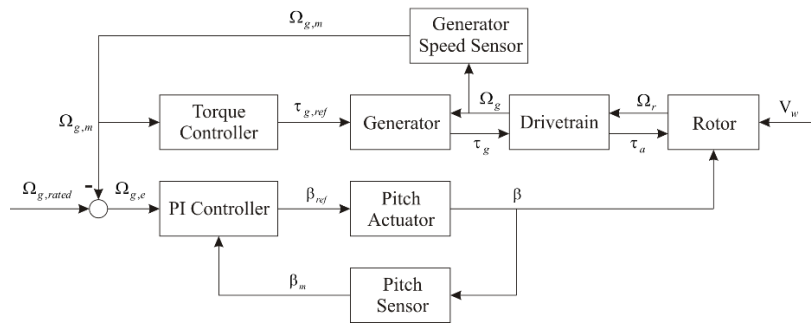


Figure 2. Block diagram of the baseline control system

2.2. Pitch actuator

Regulating each blade pitch angle individually, a 2nd-order pitch actuator is modeled to the 5 MW turbine model. Consider the blade pitch system that describes a blade pitch reference from the PI controller and the pitch angle measurement

$$\ddot{\beta}_i + 2\zeta\omega_n\dot{\beta}_i + \omega_n^2\beta_i = \omega_n^2\beta_{ref}, \quad i = 1, 2 \text{ and } 3 \quad (3)$$

where ω_n is the natural frequency and ζ is the damping ratio of the actuator. The parameters are $\omega_n = 11.11$ rad/s and $\zeta = 0.6$ [1].

Eq. (3) can also be represented as state space form including varying parameters as

$$\dot{\mathbf{x}}(t) = \mathbf{A}\mathbf{x}(t) + \mathbf{B}u(t) + \mathbf{w}(t)$$

or

$$\begin{bmatrix} \dot{\beta}_i(t) \\ \ddot{\beta}_i(t) \end{bmatrix} = \begin{bmatrix} 0 & 1 \\ -\omega_n^2 & -2\zeta\omega_n \end{bmatrix} \begin{bmatrix} \beta_i(t) \\ \dot{\beta}_i(t) \end{bmatrix} + \begin{bmatrix} 0 \\ \omega_n^2 \end{bmatrix} \beta_{ref,i}(t) + \begin{bmatrix} w_{i,1} \\ w_{i,2} \end{bmatrix}, \quad i = 1, 2 \text{ and } 3 \quad (4)$$

where $\mathbf{x}(t)$ and $u(t)$ are the state vector and input command by the individual blade pitch angle in the blade 1,2 and 3, respectively. \mathbf{A} and \mathbf{B} are system matrices: the state transition matrix and input matrix.

The actuator model in Eq. (4) describes the dynamic behavior between a pitch reference from the controller and the measurement of a pitch angle.

2.3. Pitch sensor

Since the turbine monitoring and control are based on sensor data during wind turbine operation, it is important that the acquired data should be accurate and reliable. A discretized control system including measurement noise is used in this paper. Measurement noise modeled as zero-mean

Gaussian distribution to the deterministic values according to the standard deviation is added to the pitch sensor model. Measurement equation for the sensor in the blade 1, 2 and 3, respectively is represented by a state space form as

$$y(t) = \mathbf{C}\mathbf{x}(t) + v(t)$$

or

$$\beta_{i,mes}(t) = \begin{bmatrix} 1 & 0 \end{bmatrix} \begin{bmatrix} \beta_i(t) \\ \dot{\beta}_i(t) \end{bmatrix} + v_{i,\beta}(t), \quad i = 1, 2 \text{ and } 3 \quad (5)$$

where $y(t)$ is the pitch angle measurement in the blade 1, 2 and 3 and \mathbf{C} is the measurement matrix.

3. Fault detection methods

Basic methods for establishing and evaluating residual are described in this section. Figure 3 shows the basic structure of model-based fault detection. Based on the input command $u(k)$ and measured output $y(k)$, states and measurements are estimated by an observer. By comparing measured and estimated values, changes of a state are identified by a threshold.

3.1. Observer design based on discrete-time space model in the blade pitch system

The continuous system (4) and (5) should be discretized for suitable numerical computing and employing observer. The discrete-time state space model of the blade pitch system with disturbance and faults in the pitch actuator and sensor can be transferred from the proposed system (4) and (5) that Euler discretization approach is applied.

$$\begin{aligned} \mathbf{x}(k+1) &= \mathbf{\Phi}\mathbf{x}(k) + \mathbf{\Psi}\mathbf{u}(k) + \mathbf{\Gamma}_f \mathbf{f}_A(k) + \mathbf{\Gamma}_d \mathbf{w}(k) \\ y(k) &= \mathbf{H}\mathbf{x}(k) + \mathbf{\Xi}_f f_S(k) + \mathbf{\Xi}_d v(k) \end{aligned} \quad (6)$$

where $\mathbf{\Phi} = \mathbf{I} + \mathbf{A}T$ and $\mathbf{\Psi} = \mathbf{\Gamma}_f = \mathbf{B}T$. Here, $\mathbf{\Phi}$, $\mathbf{\Psi}$, \mathbf{H} , $\mathbf{\Gamma}_d$, $\mathbf{\Gamma}_f$, $\mathbf{\Xi}_d$ and $\mathbf{\Xi}_f$ are known constant matrices in a discretized system. T is sampling time. The sensor noise is given as the uncertain disturbance including the process noise vector $\mathbf{w}(k)$ and measurement noise $v(k)$. Regarding faults, $\mathbf{f}_A(k)$ and $f_S(k)$ are the actuator fault vector and sensor fault value, respectively.

The observer with fault-free case based on Kalman filter is designed as follows,

$$\begin{aligned} \hat{\mathbf{x}}(k+1) &= \mathbf{\Phi}\hat{\mathbf{x}}(k) + \mathbf{\Psi}\mathbf{u}(k) + \mathbf{K}(y(k) - \mathbf{H}\hat{\mathbf{x}}(k)) \\ \hat{y}(k) &= \mathbf{H}\hat{\mathbf{x}}(k) \end{aligned} \quad (7)$$

where $\hat{\mathbf{x}}(k)$, $\hat{y}(k)$ and \mathbf{K} are the estimated state vector, estimated output and Kalman gain matrix.

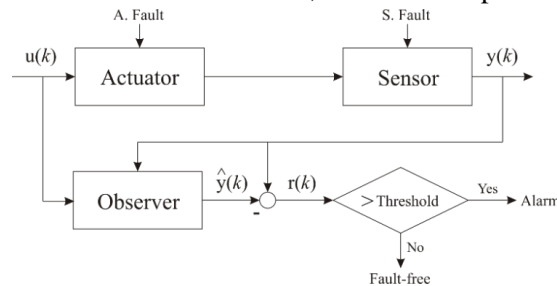


Figure 3. Scheme of observer-based fault diagnosis in the blade pitch system

3.2. Fault modelling

A pitch actuator is internally controlled by a pitch controller connected to a pitch sensor. A fault occurring in pitch system can influence the closed-loop control system and the dynamics of a wind turbine. Faults of the blade pitch system are mainly categorized by the pitch sensor and actuator fault.

The pitch sensor fault occurs by dust on encoder disc, miss-adjustment of the blade pitch bearing, beyond acceptable range of temperature and humidity or improper calibration. These causes can result in the unbalanced rotation of the rotor from the sensor bias and fixed outputs from last measurements.

The fault-free sensor is modeled as

$$\beta_{mes}(k) = \beta(k) + v(k) \tag{8}$$

Bias (PSB) can be represented by a constant offset value that is added to the measurement from the sensor

$$\beta_{mes}(k) = \beta(k) + \beta_{bias}(k) + v(k) \tag{9}$$

where $\beta_{bias}(k)$ is the pitch bias angle.

Fixed output (PSF) of sensor is that keeps the last measurement after the fault occurrence described as

$$\beta_{mes}(k) = \beta_{fixed}(k) \tag{10}$$

where $\beta_{fixed}(k)$ is the pitch after the fault.

The stuck actuator (PAS) is mainly due to valve blockage in a hydraulic pitch actuator system. Once one of the valves is blocked, the piston cannot move in pitch actuator and the ability to pitch the blade. This stuck actuator is described as

$$\beta(k+1) = \beta_{SA}, \dot{\beta}(k+1) = 0 \tag{11}$$

where β_{SA} is the pitch angle for the stuck actuator.

These faults for the blade pitch sensor and actuator frequently appear and result in structural loading of the turbine due to rotor imbalance and affect the stability of the floating platform.

Modeling the faults in the system, the state space model for the blade pitch system (6) should be updated. Table 1 describes the fault vectors in the actuator and values in the sensor. If a fault occurs in the pitch system, the fault value is applied in the pitch system equation in this algorithm.

Table 1. Mathematical model of faults applied in numerical simulations

Location	Type	Fault value
Sensor	Biased output (PSB)	$\mathbf{f}_A(k) = 0, f_S(k) = \beta_{Bias}$
	Fixed output (PSF)	$\mathbf{f}_A(k) = 0, f_S(k) = -\beta(k) + \beta_{fixed} - v(k)$
Actuator	Stuck (PAS)	$\mathbf{f}_A(k) = \begin{bmatrix} -\beta(k) - T\dot{\beta}(k) + \beta_{AS} - w_1(k) \\ (\omega_n^2\beta(k) + 2\zeta\omega_n\dot{\beta}(k) - \omega_n^2\beta_{ref}(k))T - w_2(k) \end{bmatrix}, f_S(k) = \beta_{Bias}$

3.3. Residual generation and evaluation

A residual $r(k)$ is difference between the measured and estimated values described as

$$r(k) = y(k) - \hat{y}(k) \tag{12}$$

A residual energy $J(k)$ is defined by L_2 norm which is described by root-mean-square (RMS) of residual as

$$J(k) = \|r(k)\|_2 = \left(\int_{k_1}^{k_2} r^T(k)r(k)dk \right)^{1/2} \tag{13}$$

Since the residual energy in fault cases includes fault information, the generated residual energy should be evaluated by fault detection logic. The residual determines the fault status by applying fault detection logic with threshold J_{th} in Eq. (14).

$$\begin{aligned} J(k) < J_{th}, & \text{ fault - free} \\ J(k) > J_{th}, & \text{ fault} \end{aligned} \tag{14}$$

The threshold is generated with the uncertainty that is bounded. Hence, while the residual energy is less than this threshold, the fault-free state can be indicated. Otherwise, the fault can be detected.

3.4. Threshold design

Since residual energy defined by RMS of the residual is used for fault detection, H_2 norm could be used for threshold design. H_2 norm gives a characterization of the RMS-value of the system response to uncertain inputs. However, H_∞ norm is more fundamental norm for systems and provides a measure of a worst-case system gain. H_∞ optimization is a robust method considered various uncertainties, especially disturbance. It also measures the maximum effect of the disturbances on the residual. H_∞ optimization problems are frequency-domain oriented as described in (15)

$$H_\infty = \|\mathbf{G}_{rd}(z)\|_\infty = \sup_{\omega} (\mathbf{G}_{rd}(j\omega)) \quad (15)$$

where $\mathbf{G}_{rd}(z)$ is disturbance transfer function.

As described in (16), residual energy $J(k)$ is consisted of $r_d(k)$ and $r_f(k)$.

$$J(k) = \|r_d(k) + r_f(k)\|_2 \quad (16)$$

where $r_d(k)$ and $r_f(k)$ are residuals in disturbance and fault, respectively.

If the system is a fault-free state, $r_f(k)$ should be zero. Then the residual energy is expressed as

$$J(k) = \|r_d(k)\|_2 \leq \|\mathbf{G}_{rd}(z)\|_\infty \|v\|_2 \leq \gamma_{\min} \delta_d \quad (17)$$

where the residual energy is bounded by $\|\mathbf{G}_{rd}\|_\infty \|v\|_2$. γ_{\min} is determined in Appendix A with more details for the derivation of the threshold.

Therefore, the threshold is set as

$$J_{th} = \gamma_{\min} \delta_d \quad (18)$$

4. Simulation results and discussion

In this section, a series of simulation results are presented where one blade has faults in the pitch sensor and actuator. The results prove the performance of the fault detection technique under different fault scenarios with the baseline controller. Simulations for the wind turbine subjected to a stochastic wind speed are conducted under three different fault conditions: bias (PSB), fixed output (PSF) in sensors, and a stuck actuator (PAS). For these three cases, blade 3 is subjected to a fault at 200s.

4.1. Wind modelling

Wind turbines operate under variable wind conditions such as a stochastic wind model presenting realistic winds. Turbsim [11] which is the turbulent wind simulator is used to generate realistic turbulent wind model and to test the turbine controllers in a more realistic scenario in this study. The wind model is based on the IEC 61400-3 design code. The stochastic wind data have the following characteristics in Table 2. As shown in Figure 4 that the range of the stochastic wind (12 – 24.2 m/s) covers the Region III, as its values range from 11.4 m/s up to the maximum of 25 m/s.

Table 2. Turbulent wind characteristics

Turbulence model	Kaimal's model
IEC wind type	NTM
Wind profile type	Power law profile
Grid size	160 × 160
Reference height	90m
Mean wind speed	17 m/s
Surface roughness length	0.0003 m

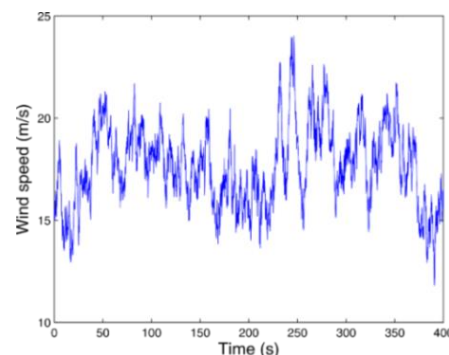


Figure 4. Wind speed measured at hub height

4.2. Effects of sensor and actuator faults

This section studies effects of faults in pitch sensors and actuators. Figure 5 shows simulation results in comparison with the pitch angle reference and measurement from a faulted blade. Each simulation has a duration of 400s where the first 200s shows the fault-free operation of the wind turbine. After 200s, sensor measurement difference caused by pitch sensor and actuator faults starts to occur. In PSB, an offset value (-3°) takes place between the reference and measurement corresponding to pitch bias. In the case of a PSF and a PAS, the pitch angle measurement shows a constant value that is the same amount of last measurement value before faults. The blade is seized that cannot respond to the change in the wind speed in the PAS case. However, a blade still operates as the pitch reference command in the PSF case that results in oscillating pitch angle. The difference between reference and measurement values makes the pitch angle oscillate irregularly with a large amplitude. Also, it makes pitch angle difference between a fault-free (blade 1, 2) and faulty (blade 3) blade.

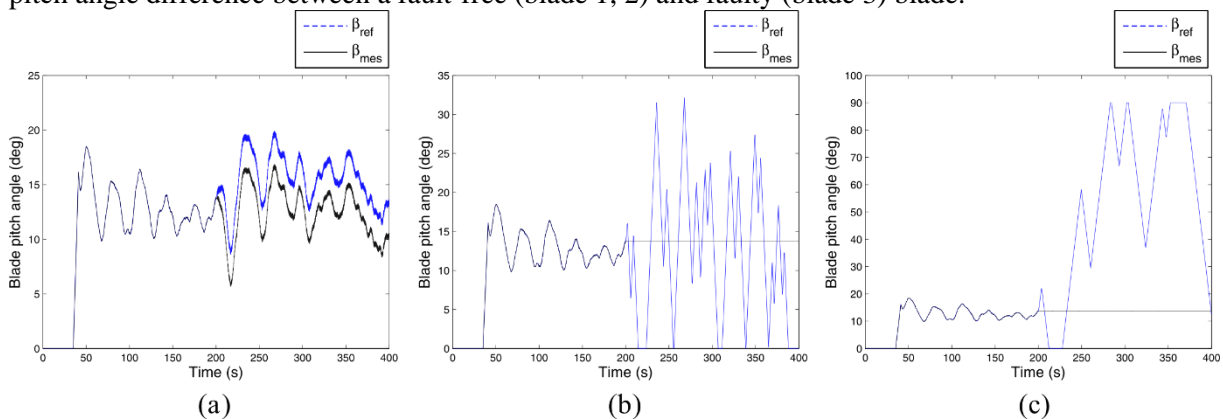


Figure 5. Comparison between pitch reference and measurement in the faulty blade (Blade 3) pitch corresponding (a) Sensor bias, (b) Fixed output in sensor and (c) Stuck actuator

Figure 6 shows a pitch angle difference between a fault-free (blade 1) and faulty (blade 3) blade corresponding to a PSB, PSF, and PAS. The incorrect pitching of a blade due to sensor measurement difference causes asymmetry forces on blades affecting the rotor introducing an unbalanced rotation. It means that a fault occurred in sensors and actuators can affect rotor dynamics and platform motions of wind turbines.

Figure 7 shows the changes of rotor speed, aerodynamic thrust, and platform yaw motion in a wind turbine due to PSB, PSF, and PAS after 200s. Incident variations in an aerodynamic thrust due to an unstable rotor speed directly affect instability of platform motions, especially a yaw motion. A PSF fault has a largest effect on dynamic behaviors compared with PSB and PAS because the magnitude of changes in aerodynamic thrust and platform yaw motion is highly increased. It concludes that structural loads are dangerously increased on the rotor, drivetrain or tower of the wind turbine.

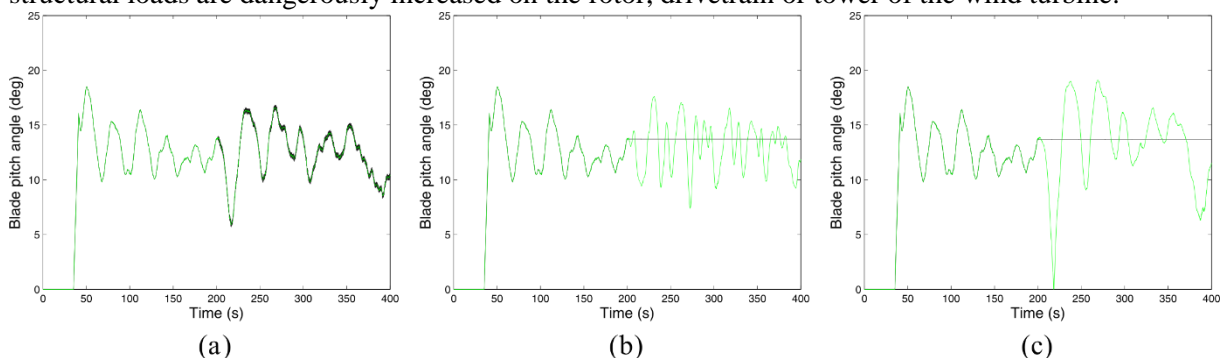


Figure 6. Measured pitch angles using sensors in fault-free (blade 1, green) and faulted (blade 3, black) blade pitch system under different fault cases corresponding (a) PSB, (b) PSF and (c) PAS

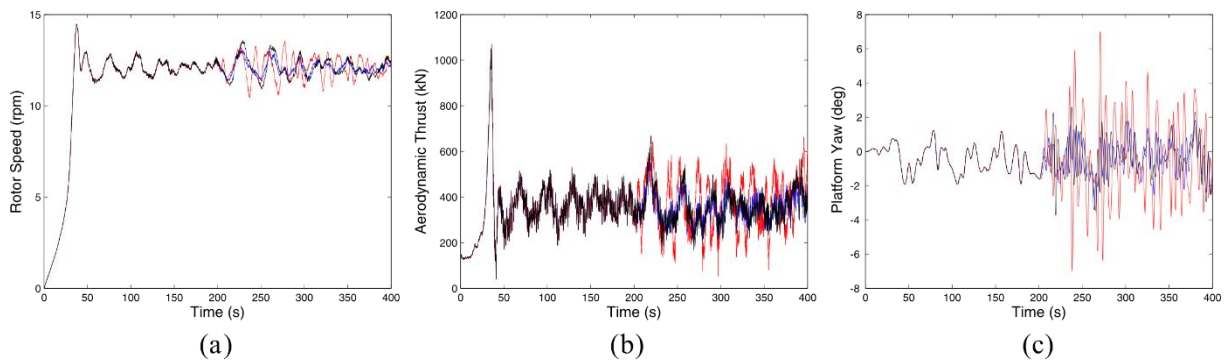


Figure 7. Effect of faults on (a) rotor speed, (b) aerodynamic thrust and (c) platform yaw motion under different fault cases corresponding PSB (blue), PSF (red) and PAS (black)

4.3. Fault detection results

Fault detection for the blade pitch system takes into account the faults that influence dynamics of the wind turbine. Faults in actuators and sensors can be detected effectively by the residual energy and the threshold. When the residual energy is greater than the threshold, a fault alarm is set to 1 which means that a fault is detected. The residual energy should be normalized to adjust scale factor from data. The normalized residual energy J_N is described as

$$J_N(t) = J(t) / J_{th} \tag{19}$$

Figure 8 shows simulation results in connection with the blade pitch angle, normalized residual energy, and fault alarm. In Figure 8 (a), a blade pitch sensor bias value gradually occurs during 10s after 200s in the wind turbine corresponding to a sensor bias of -3° on blade 3. At the same time, the normalized residual exceeds the threshold, and then the observer detects the blade pitch bias fault immediately by setting to fault alarm in Figure 8 (b) and (c), respectively.

Simulation results on PSF and PAS show the same pattern as well in Figures 9 and 10, respectively. These are illustrated that it is possible to detect a pitch offset on a blade 3 based on the fault detection algorithm.

For reliability of this fault detection algorithm, 15 simulations runs are conducted for mean wind speeds from 11 to 25 m/s as an increment of 1m/s. As listed in Table 3, average fault detection time in sensor and actuator faults is within 4 seconds after fault generated. It means that this method can guarantee the fault detection at the early stage in the blade pitch system.

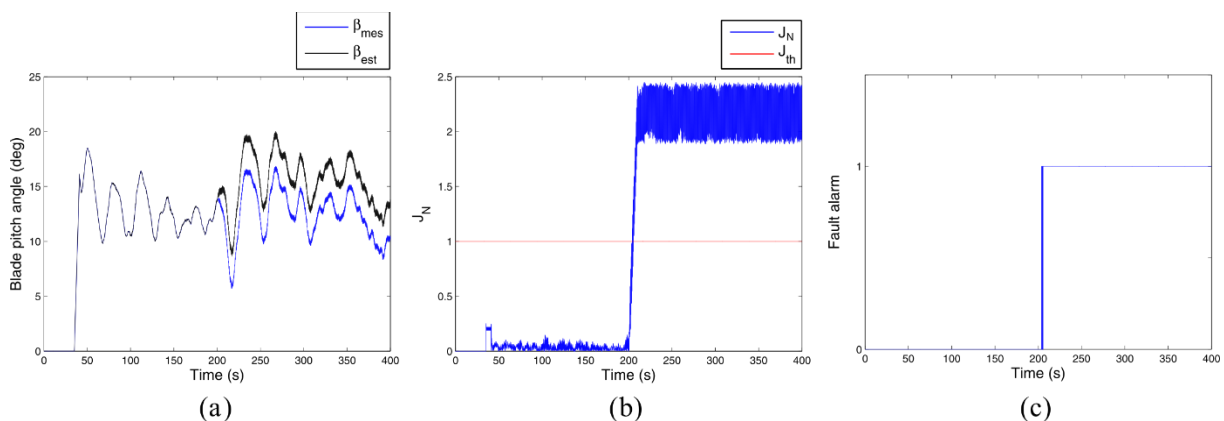


Figure 8. Simulation results of the PSB case corresponding the blade pitch angle: (a) pitch angle measurement (blue) and estimation (black), (b) normalized residual energy and (c) fault alarm

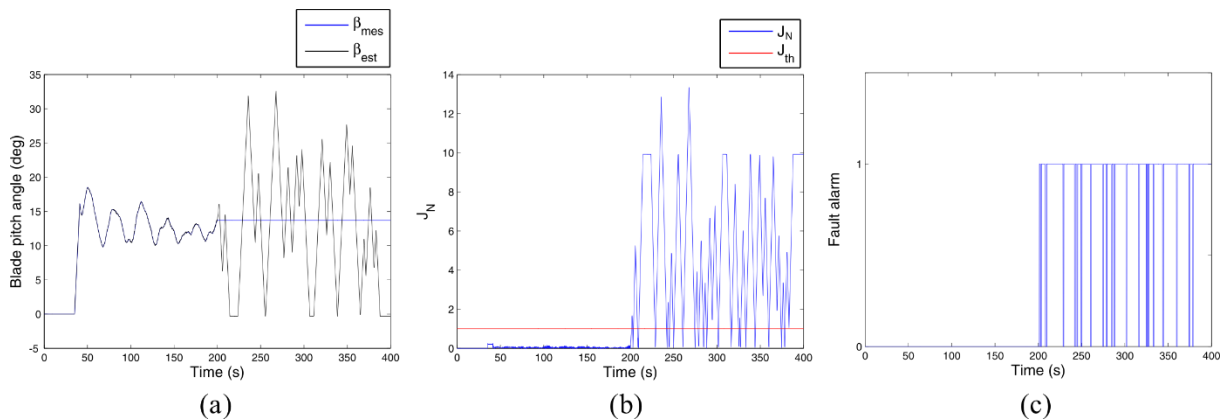


Figure 9. Simulation results of the PSF case corresponding the blade pitch angle: (a) pitch angle measurement (blue) and estimation (black), (b) normalized residual energy and (c) fault alarm

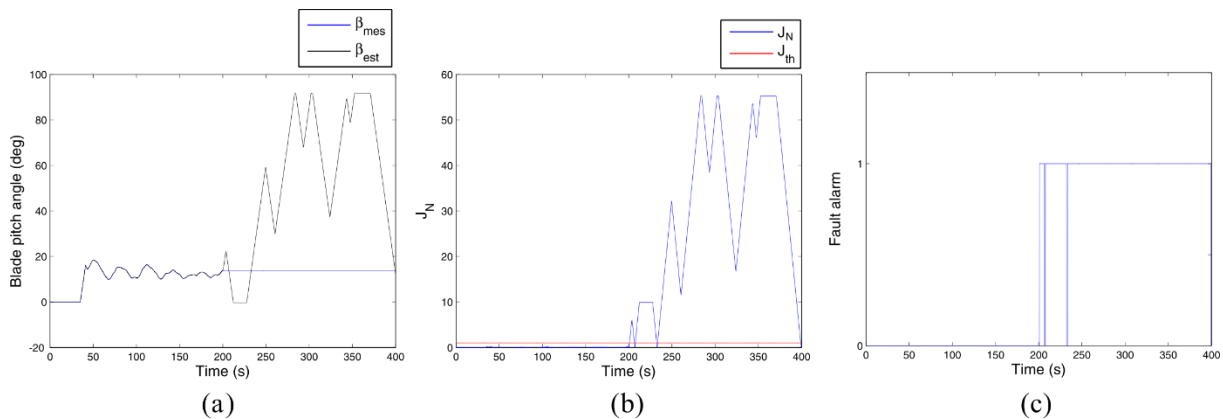


Figure 10. Simulation results of the PAS case corresponding the blade pitch angle: (a) pitch angle measurement (blue) and estimation (black), (b) normalized residual energy and (c) fault alarm

Table 3. Detection time of each fault after fault occurrence

Location	Type	Average detection time
Sensor	Biased output	3.7s
	Fixed output	1.3s
Actuator	Stuck	1.1s

5. Conclusion

Faults in the floating wind turbine should be detected at the early stage to prevent catastrophic failures. The fault detection method is suggested based on an observer designed by Kalman filter focus on the blade pitch actuator and sensor faults. In a model-based approach, it is typical that a fault is detected by residual signal and threshold. A Kalman filter is used for residual generation, and H_∞ norm and an LMI technique are used to set a threshold for residual evaluation for detecting faults in blade pitch actuators and sensors. The proposed method is shown to detect all three faults in a case study that bias and fixed output in pitch sensors and stuck in pitch actuators at the early stage. In the future, an algorithm to decide more accurate by the fault status to isolate described faults in the blade pitch system will be addressed. It can be used in the fault-tolerant control to avoid propagating damages in the floating wind turbine.

Appendix A. Threshold design

A1. Residual generator in frequency domain

Remember that for the state space form (4); the residual generator can be realized as a composition of Kalman filter (7). It transforms by setting $\mathbf{e}(k) = \mathbf{x}(k) - \hat{\mathbf{x}}(k)$, the residual system equations can be re-written as

$$\begin{aligned}\mathbf{e}(k+1) &= \bar{\Phi}\mathbf{e}(k) + \bar{\Gamma}_d\mathbf{w}(k) + \bar{\Gamma}_f\mathbf{f}_A(k) \\ r(k) &= \mathbf{H}\mathbf{e}(k) + \bar{\Xi}_d v(k) + \bar{\Xi}_f f_S(k)\end{aligned}\quad (20)$$

Where $\bar{\Phi} = \Phi - \mathbf{K}\mathbf{H}$, $\bar{\Gamma}_d = \Gamma_d - \mathbf{K}\Xi_d$ and $\bar{\Gamma}_f = \Gamma_f - \mathbf{K}\Xi_f$.

Residual generator also can be defined in frequency domain as

$$r(z) = r_d(z) + r_f(z) = \mathbf{G}_{rd}(z)v(z) + \mathbf{G}_{rf}(z)f(z)\quad (21)$$

where $\mathbf{G}_{rd}(z) = \mathbf{H}(z\mathbf{I} - \bar{\Phi})^{-1}\bar{\Gamma}_d + \bar{\Xi}_d$ and $\mathbf{G}_{rf}(z) = \mathbf{H}(z\mathbf{I} - \bar{\Phi})^{-1}\bar{\Gamma}_f + \bar{\Xi}_f$. $\mathbf{G}_{rd}(z)$ is the disturbance transfer function, and $\mathbf{G}_{rf}(z)$ is the fault transfer function.

A2. Linear matrix inequality (LMI) in a discrete-time system

Consider a system (6) and observer (7). For a given constant $\gamma > 0$, system (6) is asymptotically stable and satisfies

$$\|G_d(z)\|_{\infty} \leq \gamma\quad (22)$$

There exists a matrix K and a symmetric matrix $P > 0$ such that

$$\begin{bmatrix} \bar{\Phi}^T P \bar{\Phi} - P + \mathbf{H}^T \mathbf{H} & \bar{\Phi}^T P \bar{\Gamma}_d + \mathbf{H}^T \bar{\Xi}_d \\ \bar{\Xi}_d^T \mathbf{H} & \bar{\Xi}_d^T \bar{\Xi}_d + \bar{\Gamma}_d^T P \bar{\Gamma}_d - \gamma^2 \mathbf{I} \end{bmatrix} < 0\quad (23)$$

where γ is a design parameter named as the performance bound.

References

- [1] Esbensen T and Sloth C 2009 *Fault diagnosis and fault-tolerant control of wind turbines* (Master's thesis: Aalborg University) p 167
- [2] Zhang Y, Wu L, Li J and Chen X 2012 LMI approach to mixed H_2/H_{∞} fault detection observer design *Transactions of Tianjin University* **18** pp 343-349
- [3] Odgaard P F, Stoustrup J and Kinnaert M 2009 Fault-tolerant Control of Wind Turbines - a benchmark model, *Proceedings of the 7th IFAC Symposium on Fault Detection, Supervision and Safety of Technical Processes* (Barcelona: Spain) pp 155 - 160
- [4] Chen W, Ding S X, Haghani A, Naik A, Khan A Q and Yin S 2011 Observer-based FDI Schemes for Wind Turbine Benchmark *Proceedings of the 18th IFAC World Congress* (Milano: Italy) pp 7073 - 7078
- [5] Wang L, Wu L, Guan Y and Wang G 2015 Online Sensor Fault Detection Based on an Improved Strong Tracking Filter *Sensors* **15** pp 4578-4591
- [6] Jonkman J, Butterfield S, Musial W and Scott G 2009 Definition of a 5-MW reference wind turbine for offshore system development *Technical Report NREL/TP-500-38060* (USA) p 63
- [7] Jonkman J 2010 Definition of the floating system for Phase IV of OC3 *Technical Report NREL/TP-500-47535* (USA) p 31
- [8] Bachinski E 2014 Simo-Riflex-Aerodyn manual *MARINTEK Technical Report* (Norway) p 51
- [9] Larsen TJ and Hanson TD 2007 A method to avoid negative damped low-frequency tower vibration for a floating, pitch controlled wind turbine *Journal of Physics Conference Series* **75** pp 12-73
- [10] Etemaddar M, Blanke M, Gao Z and Moan T 2016 Response analysis and comparison of a spar-type floating offshore wind turbine and an onshore wind turbine under blade pitch controller faults *Wind energy* **19** pp 35-50
- [11] Jonkman J and Kilcher L 2012 TurbSim User's Guide *Technical Report NREL* (USA) p76